nature photonics

SUPPLEMENTARY INFORMATION

DOI: 10.1038/NPHOTON.2017.96

In the format provided by the authors and unedited.

Planar metasurface retroreflector

Amir Arbabi,[1] Ehsan Arbabi,[1] Yu Horie,[1] Seyedeh Mahsa Kamali,[1] and Andrei Faraon[1]

[1]*T. J. Watson Laboratory of Applied Physics, California Institute of Technology, 1200 E California Blvd., Pasadena, CA 91125, USA*

SUPPLEMENTARY FIGURES

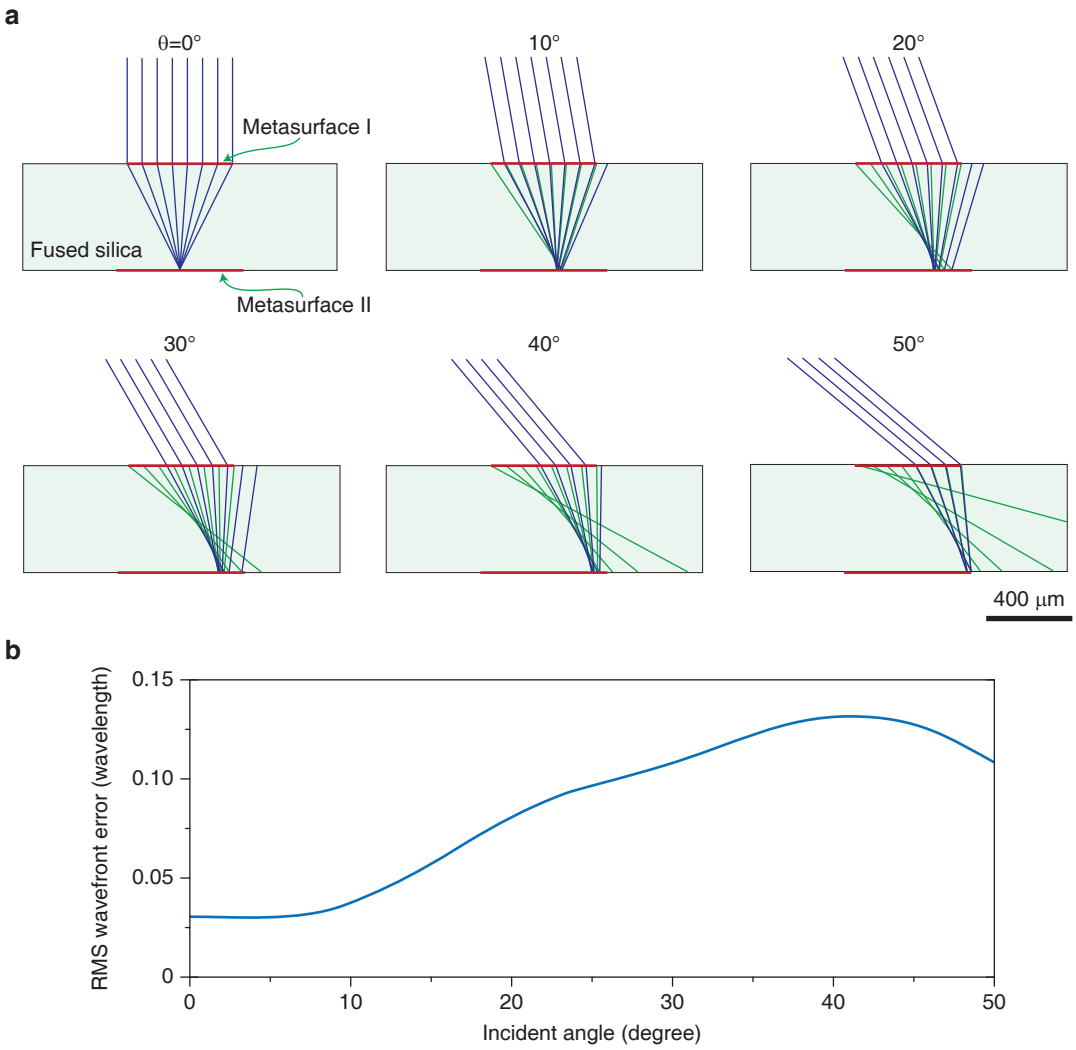

Supplementary Figure 1 | Simulation results of the planar retroreflector. **a**, Ray diagram for different incident angles. The incident rays (green) are not shown outside the substrate so that the reflected rays (dark blue) are seen more clearly. **b**, Root mean square (RMS) wavefront error of the retroreflected light as a function of the incident angle.

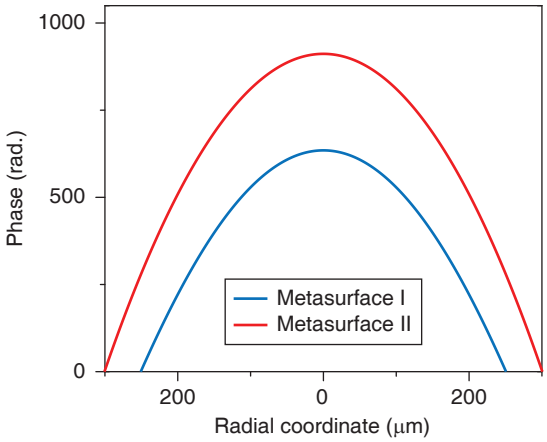

Supplementary Figure 2 | Phase profiles of the metasurfaces composing the planar retroreflector. Optimized phase profiles of the metasurfaces that minimize the average RMS wavefront error (see Supplementary Fig. 1).

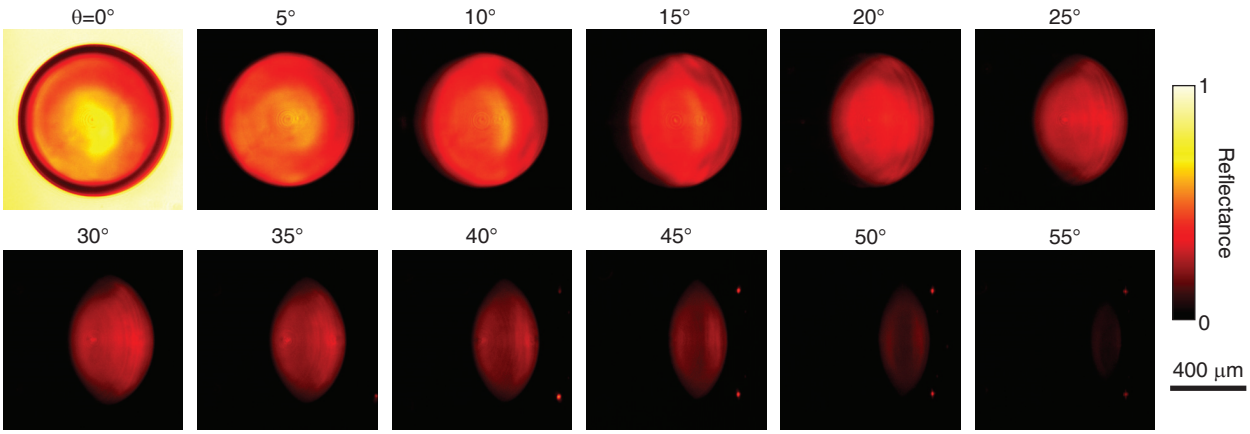

Supplementary Figure 3 | Extended reflectance measurement results. The results are the same as the ones shown in Fig. 4a, but are presented here in 5° steps.

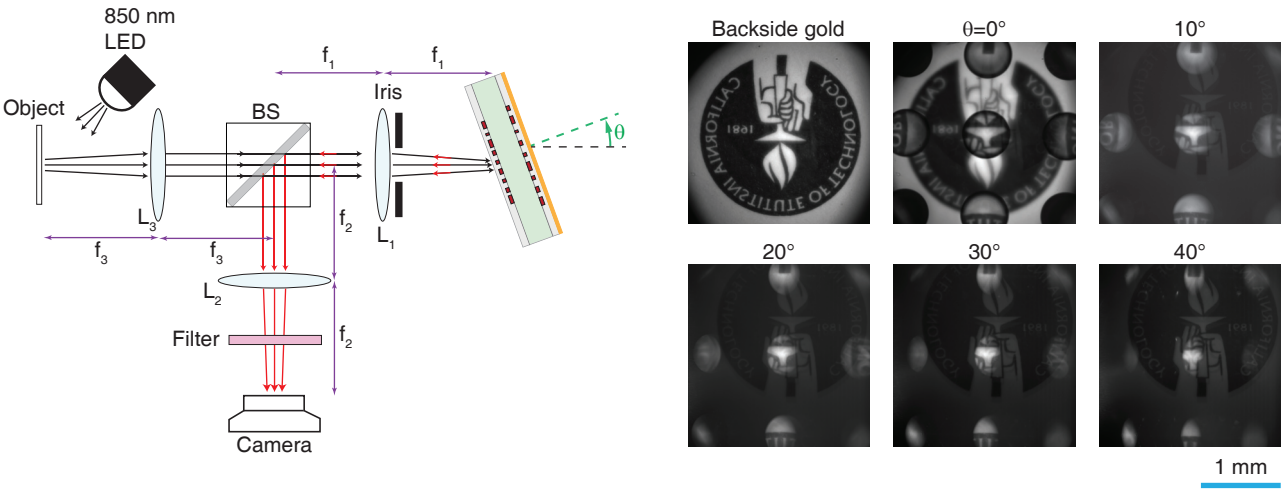

Supplementary Figure 4 | Retroreflected images captured using a lens with long depth of focus. Schematic of the measurement setup (left), and images of the object in the backside gold mirror and in the retroreflector for different retroreflector rotation angles (right). The setup is similar to the one shown in Fig. 5a, except for the objective lens replaced with a low numerical aperture lens, and a lager object. The numerical aperture of L_1 is 0.08 and its depth of focus is approximately 130 μm. The relatively long depth of focus of L_1 allows for simultaneously observing both the retroreflected and reflected images of the object in the $\theta = 0$ image (i.e. normal incidence). The faint images observed in the background for 10° to 40° are due to undesirable reflection from the output side of the beam splitter cube and they exist even when the device is removed from the setup. BS: beam splitter cube, L: lens. The focal lengths of lenses L_1 and L_2 are f_1=3 cm and f_2=20 cm, respectively. The diameter of the iris aperture is set to 5 mm.

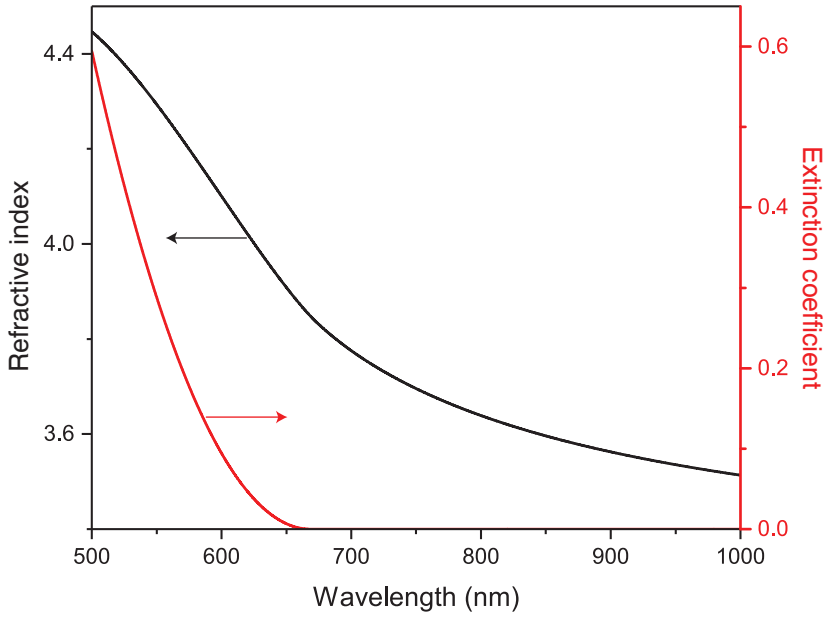

Supplementary Figure 5 | Refractive index of amorphous silicon. Measured refractive index and extinction coefficient of amorphous silicon deposited at 200°C using plasma enhanced chemical vapor deposition. The index values are measured using a variable angle spectroscopic ellipsometer.

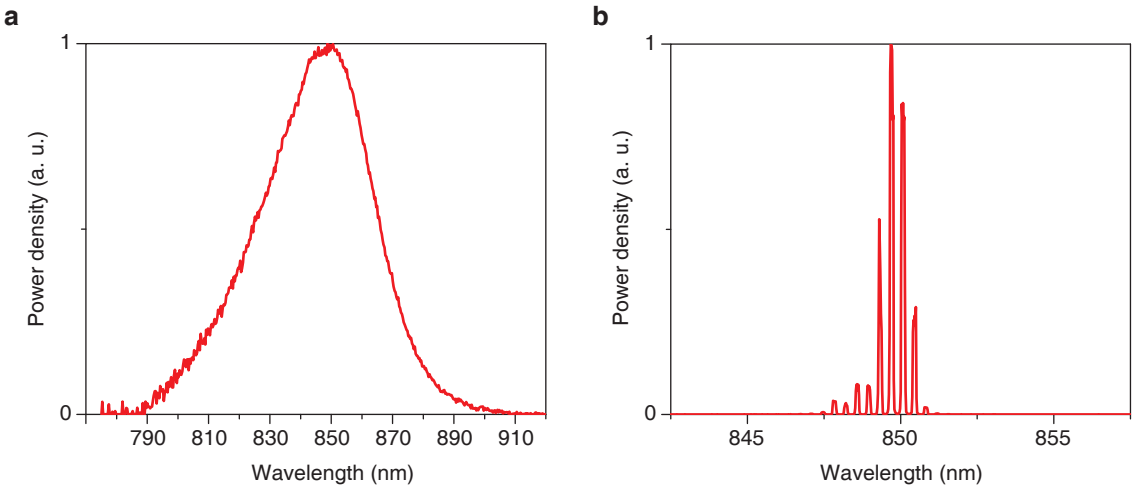

Supplementary Figure 6 | Spectra of sources used for the retroreflector characterization. a, Measured spectrum of the LED used in the measurement shown in Fig. 4a. **b**, Measured spectrum of the laser used in retroreflection efficiency measurement (Fig. 4b). The full width at half maximum bandwidth values for the best Gaussian fits to the spectra shown in (**a**) and (**b**) are 42.7 nm and 0.9 nm, respectively.

SUPPLEMENTARY TABLES

Supplementary Table 1 | Phase profile parameters for the metasurfaces composing the retroreflector

Metasurface	R (μm)	a_1	a_2	a_3	a_4	a_5	a_6	a_7
Metasurface I	250	-669.15	33.67	0.32	6.61	-3.77	1.11	-0.12
Metasurface II	300	-903.33	-9.03	6.47	-2.85	0.67	-0.08	0.00

SUPPLEMENTARY VIDEO LEGENDS

Supplementary Video 1 | Reflectance of the retroreflector. Measured reflectance of the metasurface retroreflector as the angle between the retroreflector normal and the incident light (θ) is increased from 0° to 55°.